FERMILAB-CONF-09-287-E

Validation of Broadly Filtered Diagonalization Method for Extracting Frequencies and Modes from High-Performance Computations

T. M. Austin[1], J. R. Cary[1,2], G. R. Werner[2] and L. Bellantoni[3]

[1]Tech-X Corporation, 5621 Arapahoe Ave., Boulder, CO 80303, USA
[2]Center for Integrated Plasma Studies, University of Colorado, Boulder CO 80309, USA
[3]Fermi National Accelerator Laboratory, Batavia, IL, 60510, USA

E-mail: `austin@txcorp.com`

Abstract. Recent developments have shown that one can get around the difficulties of finding the eigenvalues and eigenmodes of the large systems studied with high performance computation by using broadly filtered diagonalization [G. R. Werner and J. R. Cary, J. Comp. Phys. 227, 5200 (2008)]. This method can be used in conjunction with **any** time-domain computation, in particular those that scale very well up to 10000s of processors and beyond. Here we present results that show that this method accurately obtains both modes and frequencies of electromagnetic cavities, even when frequencies are nearly degenerate. The application was to a well-characterized Kaon separator cavity, the A15. The computations are shown to have a precision to a few parts in 10^5. Because the computed frequency differed from the measured frequency by more than this amount, a careful validation study to determine all sources of difference was undertaken. Ultimately, more precise measurements of the cavity showed that the computations were correct, with remaining differences accounted for by uncertainties in cavity dimensions and atmospheric and thermal conditions. Thus, not only was the method validated, but it was shown to have the ability to predict differences in cavity dimensions from fabrication specifications.

1. Introduction

Electromagnetic cavities are essential to many high-energy physics experiments. They can be tuned to deliver a desired performance by adjusting physical parameters like shape, curvature, and size. Yet, it is a non-trivial task to determine the dependency of such physical parameters on cavity performance. Also, usage of expensive metals such as niobium means design errors can be particularly costly. Coupled with the knowledge that fabrication cannot deliver exact specifications, it is critical to perform computational studies to assist in cavity design and avoid design errors.

Finite element simulations are presently used to compute frequencies and eigenmodes of electromagnetic cavities within the US Department of Energy's science program [1]. Recently, a novel approach that uses the Finite-Difference Time-Domain (FDTD) method applied to Maxwell's equations for computation of frequencies and eigenmodes of electromagnetic cavities was reported [2]. The standard approach to using the FDTD method applied to Maxwell's equations for frequency extraction is to use narrowly-filtered states combined with post-simulation FFTs. The limitations of this approach are that it cannot account for degenerate

frequencies or reconstruct spatial mode patterns. The new broadly filtered *Filter Diagonalization Method* (FDM) presented by Werner and Cary in [2] overcomes these limitations.

We present validation results for the broadly filtered FDM applied to a 3.9 GHz Kaon separator fabricated at Fermilab in 1999. Previously, experimental frequency measurements obtained from bead pull experiments were reported in [3] in addition to computational frequency measurements obtained using the Finite Integration Technique. We show here that calculations using the VORPAL computational framework [4] along with the broadly filtered FDM predicted differences in cavity dimensions from fabrication specifications.

2. Broadly-Filtered FDM

The second-order form of Maxwell's equations,

$$-\frac{\partial^2}{\partial t^2}\mathbf{E}(x,y,z,t) = \nabla \times \nabla \times \mathbf{E}(x,y,z,t) = L\mathbf{E}(x,y,z,t), \tag{1}$$

permits the eigenvalue problem for $\nabla \times \nabla\times$ to be viewed as an eigenvalue problem for the second-order time evolution operator. The standard approach to finding the eigenspace of the $\nabla \times \nabla\times$ operator is to work directly with a discretized form of $\nabla \times \nabla\times$ whereby a large scale eigenvalue problem, $\mathbf{A}\vec{x} = \lambda\vec{x}$, generated from, e. g., the finite element method is solved [1].

The broadly filtered FDM is based on the concept that L can be transformed into block-diagonal form with one large block filtered out and the remaining small block diagonalized by the singular value decomposition (SVD). The eminently scalable FDTD method is employed along with targeted excitations that excite eigenmodes inside of a range of interest. The Dey-Mittra boundary algorithm [5] is employed to model the curved domains that arise in electromagnetic cavities.

To excite the modes inside the frequency range $[\omega_L, \omega_U]$, we define a time-varying current as $\mathbf{J}(x,y,z,t) = g(t)\hat{\mathbf{J}}(x,y,z)$ given that

$$g(t) = \begin{cases} 2\left[\frac{\sin(\omega_L(t-T/2))}{t-T/2} - \frac{\sin(\omega_U(t-T/2))}{t-T/2}\right]\exp^{-\sigma_\omega^2(t-T/2)^2/2} & 0 \le t \le T, \\ 0 & \text{otherwise} \end{cases} \tag{2}$$

and $\hat{\mathbf{J}}(x,y,z)$ is a spatial field that promotes extraction of the eigenmodes. This current is applied to Maxwell's equations as

$$\begin{aligned} \frac{\partial \mathbf{B}(x,y,z,t)}{\partial t} &= -\nabla \times \mathbf{E}(x,y,z,t) \\ \frac{\partial \mathbf{E}(x,y,z,t)}{\partial t} &= -\nabla \times \mathbf{B}(x,y,z,t) - \mathbf{J}(x,y,z,t). \end{aligned} \tag{3}$$

The parameter σ_ω in Eq. (2) is calculated via the distance of the frequency nearest to the frequency range $[\omega_L, \omega_U]$. Also, if a K-degeneracy exists, then K different spatial patterns, $\hat{\mathbf{J}}$, are used yielding K simulations to extract the K-degeneracy.

The targeted excitation acts as the filtering component of the broadly filtered FDM. Small scale linear algebra is then employed for a small scale eigenvalue problem that only requires minutes to solve on a single CPU core. This is in contrast to the large scale eigenvalue problem discussed above that demands 10000s of cores and significant run time. In the method discussed here, the bulk of the work goes into running the FDTD simulations out to time T, during which time the fields are sampled to construct the small scale eigenvalue problem.

We now briefly describe the generation of the small scale eigenvalue problem. The reader can refer to [2] for more details. Once the simulation is ran to time T, the field of interest (either the electric field or the magnetic field) is sampled during the next few cycles at P grid points and at L times. Referring to these sampled discrete fields as $\mathbf{s}_\ell$, we construct the relationship,

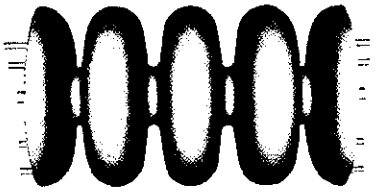

Figure 1. A side view of the 3.9 GHz A15 crab cavity that was fabricated in 1999 for the development of a separated K^+ beam.

$\mathbf{r}_\ell = L\mathbf{s}_\ell$ where L denotes taking the second-order time derivative of the $\mathbf{s}_\ell$. We then recognize that any eigenvector $\mathbf{v}_m$ can be expressed as

$$\mathbf{v}_m = \sum_{\ell=1}^{L} a_{m,\ell}\mathbf{s}_\ell, \tag{4}$$

and that the application of L yields

$$\lambda_m \mathbf{v}_m = \sum_{\ell=1}^{L} a_{m,\ell}\mathbf{r}_\ell. \tag{5}$$

We then have the generalized eigenvalue problem

$$R\mathbf{a}_m = \lambda_m S\mathbf{a}_m, \tag{6}$$

where the number of columns of R and S correspond to L and the number of rows corresponds to P. Instead of solving Eq. (6) we solve the generalized eigenvalue problem

$$S^\dagger R\mathbf{a}_m = \lambda_m S^\dagger S\mathbf{a}_m, \tag{7}$$

using the SVD for $S^\dagger S = VD^2V^\dagger$, where D is diagonal and V is orthogonal. The eigenvalues are related to frequencies by $\omega_m = \sqrt{\lambda_m}/2\pi$ and the eigenvectors of Eq. (7) represent coefficients used in reconstructing the corresponding eigenmodes of Maxwell's equations.

3. A15 Cavity

3.1. Background

To validate the broadly filtered FDM, we examined a well-characterized Kaon separator cavity, the A15 cavity. This cavity, which is pictured in Fig. 1, was designed in 1999 as a Kaon separator [6]. Its shape is determined by physical parameters like the equatorial radius, iris radius, iris curvature, equatorial curvature, and cell half length. These parameter values are 47.19 mm, 15.00 mm, 3.31 mm, 13.6 mm, and 19.2 mm yielding a 3.9 GHz crab cavity. In [3], Bellantoni reported on experimental frequency measurements using bead-pull experiments and also preliminary calculations using a Finite Integration Technique. The TM_{010} deflecting modes had the experimentally-determined frequency values given in Table 1.

3.2. Initial Calculations

With a lower frequency bound of $f_L = 3902$ MHz and an upper frequency bound of $f_U = 4110$ MHz, the correct form of Eq. (2) was determined given that the separation between the frequency range, $[f_L, f_U]$, and the nearest mode was 210 MHz. The nearest mode, $\hat{f}$, at 4320 MHz

Table 1. Frequencies (in MHz) of the five TM_{010} modes of the A15 cavity. Measurements were reported in 2000 by Bellantoni in the unpublished note [3].

f_0	f_1	f_2	f_3	f_4
3902.810	3910.404	3939.336	4001.342	4106.164

Table 2. Calculated frequencies (in MHz) using Richardson extrapolation of the five TM_{010} modes of the A15 cavity using the original specifications for the A15 cavity reported in [3].

f_0	f_1	f_2	f_3	f_4
3900.512	3908.552	3937.325	4000.107	4103.616

was reduced by $h = 1e\text{-}7$ by running the excitation for at least 200 cycles at 4000 MHz. The simulation was ran for another π cycles during which time the fields were sampled. At these parameter values, the value of σ_ω in Eq. (2) was $2\pi|\hat{f} - f_U|/5.68$ and the corresponding excitation time was set to be $T = 11.4/\sigma_\omega$.

In Table 2, we present results obtained using the broadly filtered FDM and Richardson extrapolation from computational results at longitudinal resolutions from 0.533 mm to 0.267 mm, with transverse resolution arbitrarily 25% greater. A comparison of Tables 1 and 2 show that results are only accurate to 1 part in 10^4 which exceeds the computational uncertainty. Possible errors include error in the computational software, missing physics effects, and/or error in the geometrical model. Since the method had been previously verified for a rectangular cavity in [2], errors in the computational software were unlikely. Missing physics effects were found to be insufficient to account for the error so we focused on errors in the geometrical model.

3.3. Validation

In [7], the authors reported on the sensitivity of frequency values to various cavity parameters like equatorial radius, iris radius, and cell half length. The sensitivity of the frequency with respect to the equatorial radius was found to be -80.6 MHz/mm while the sensitivity to iris radius and cell half length was -25.6 MHz/mm and 17.5 MHz/mm, respectively. Knowing that a typical machining error could be 1 mil or 0.0254 mm, it seemed likely that a machining error could produce the discrepancies between computational results and experimental measurements.

Preliminary simulations were performed for an equatorial radius reduced by $\sim$ 1 mil. Results at the fundamental frequency were found to be 3902.514 MHz as compared to the original computed value of 3900.512 MHz, implying accuracy to 1 part in 10^5, which is within computational uncertainty. The results for all five frequencies are found in Table 3. As a result of these findings, a careful re-measurement of the A15 was made at Fermilab. New measurements showed that the equatorial radius was 47.165 $\pm$ 0.007 mm in contrast to the original 47.19 mm. Thus, the method predicted differences in cavity dimensions from fabrication specifications.

3.4. Mode Reconstruction

The method can also be used for reconstruction of the modes. In Fig. 2, we show a slice of the B_z component of the magnetic field for the five TM_{010} modes. The reconstruction of the modes only requires a few minutes on a single core. Fields are described in the Hierarchical Data Format (HDF5) following the VizSchema [8] conventions. This standard permits dumping of fields at arbitrary times for viewing with tools like VisIt.

Table 3. Calculated frequencies (in MHz) using Richardson extrapolation of the five TM_{010} modes of the A15 cavity. The altered specifications for the A15 cavity were used in the simulations whereby the equatorial radius was $\sim$ 1 mil smaller.

f_0	f_1	f_2	f_3	f_4
3902.514	3910.509	3939.155	4001.757	4105.940

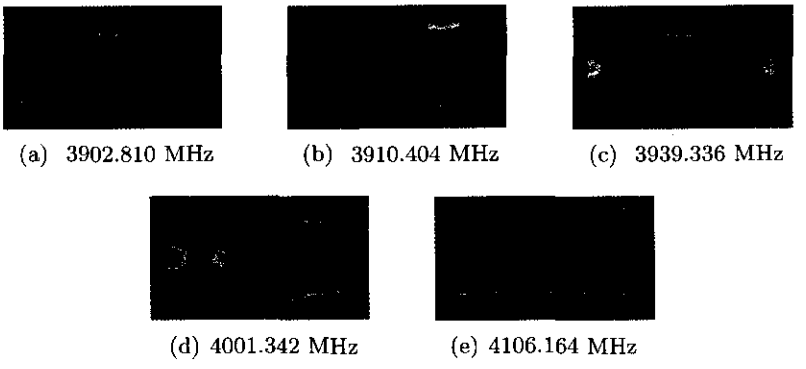

(a) 3902.810 MHz (b) 3910.404 MHz (c) 3939.336 MHz

(d) 4001.342 MHz (e) 4106.164 MHz

Figure 2. Slice of the B_z component of the magnetic field for the five TM_{010} modes of the A15 cavity. Simulations were ran at a resolution of $1.07 \times 1.3 \times 1.3$ mm^3 resulting in approximately 1.05 million grid points.

4. Summary

Validation of the broadly filtered FDM introduced in [2] was performed for the 3.9 GHz Kaon separator cavity. Original calculations revealed that the specifications were not delivered and that adjustments to the equatorial radius were needed to deliver accurate frequency calculations due to machining error. The broadly filtered FDM was also used for reconstruction of the spatial mode patterns.

5. Acknowledgements

This work was supported by the U.S. Department of Energy grants DE-FG02-04ER41317, DE-FC02-07ER41499, and DE-AC02-07CH11359.

References

[1] Ko K, Folwell N, Ge L, Guetz A, Lee L, Li Z, Ng C, Prudencio E, Schussman G, Uplenchwar R *et al.* 2006 *Physica C: Superconductivity and Its Applications* **441** 258–262

[2] Werner G and Cary J 2008 *Journal of Computational Physics* **227** 5200–5214

[3] Bellantoni L Characterization of the aluminum models of the 3.9 GHz separators for a K^+ beam at Fermilab unpublished note

[4] Nieter C and Cary J 2004 *Journal of Computational Physics* **196** 448–473

[5] Dey S and Mittra R 1997 *IEEE Microwave and Guided Wave Letters* **7** 273–275

[6] Bellantoni L, Edwards H, McAshan M and Wanzenberg R 2001 Design and measurements of a deflecting mode cavity for an RF separator *Conference: Particle Accelerator Conference, Chicago, IL (US), 06/18/2001–06/22/2001*

[7] Burt G, Bellantoni L and Dexter A 2007 *EUROTeV-Report-2007-003*

[8] VizSchema `https://ice.txcorp.com/trac/vizschema` last accessed April 16, 2009.